

Short Papers

Extremum-Seeking Nonlinear Controllers for a Human Exercise Machine

X. T. Zhang, D. M. Dawson, W. E. Dixon, and B. Xian

Abstract—In this paper, a next generation exercise machine controller is developed for a single degree of freedom (DOF) system to maximize the user's power output and ensure passivity with the user. In an effort to optimize the user's power expenditure, a desired velocity trajectory is developed that seeks the unknown user-dependent optimal velocity setpoint. Two extremum-seeking algorithms are presented (e.g., Kristic and Deng, and Tsekosky *et al.*) that seek the optimal velocity setpoint while ensuring the trajectory is sufficiently differentiable. To track the reference trajectory and to ensure passivity, two controllers are developed. The first controller is developed based on the assumption that the user's torque input can be measured. A second controller is designed that estimates the user's torque input. Both controllers are proven to ensure that the exercise machine remains passive with respect to the user's power output. The controllers are proven to yield semiglobal tracking through Lyapunov-based analyses. Proof-of-concept experimental results are provided that illustrate the performance of the torque estimation controller.

Index Terms—Exercise machine, nonlinear controller, passive controller.

I. INTRODUCTION

Generally, exercise machines are classified according to characteristics such as the source of the exercise resistance, the exercise motions, and the exercise objectives [1], [10]. Traditional exercise machines (see, e.g., [3]) do not incorporate user-specific information in the machine functionality. Typically, traditional exercise machines either rely on manual adjustment of the machine parameters (e.g., altering resistance levels) or automatic adjustment based on an open-loop approach. Exercise based on manual adjustments by the user are affected by the psychological state of the user, which may result in decreased performance. To maximize the user's power output, recent research has focused on closed-loop actuated exercise equipment that incorporates feedback from the user. That is, next generation exercise machines will incorporate user performance information to actively change the resistance. In addition to maximizing the user's power output, an additional challenge for actuated exercise machines is to maintain passivity with respect to the user.

Some research has been directed at developing these next generation exercise machines. In [2], a state-feedback controller is developed for

a human arm exercise machine. The machine described in [2] uses an actuated mechanism to give the user a sensation of moving "virtual" dynamic systems such as a mass, spring, or damper. Unfortunately, the control design in this preliminary research does not address the passivity problem or the self-optimizing problem. In [10] and [11], a passive exercise machine controller is developed. With the assumption that muscle force decreases linearly with the velocity of motion, the controller ensures tracking of an arbitrary desired velocity field and system passivity. The strategy in [10] and [11] employs a combination of an adaptive tracking controller and a reference trajectory generator. To compensate for the uncertainty in the user's biomechanics, the reference generator requires a training phase where the algorithm learns user-specific parameters. Once the user's parameters are acquired for a specific exercise session, an optimal reference trajectory is generated. In [5], an adaptive resistance controller is designed with the restriction that the resistance mechanism has only a braking capability. The static damping control design in [5] ensures the passivity of the closed-loop system to an external input force and bounded tracking errors. An optimal exercise protocol is proposed in [5] based on an assumed linear velocity dependence of human force. Identification of the nonlinear system dynamics of the exercise motions and torque output of the resistance mechanisms are used in [5] to deal with unknown human biomechanical behavior.

In this paper, a nonlinear exercise machine controller is developed for a single degree of freedom system. One goal of the exercise machine controller is to maximize the user's power expenditure. Hence, a desired trajectory signal is designed to seek the optimal velocity setpoint that will maximize the user's power output, while the controller is designed to ensure that the exercise machine tracks the resulting desired trajectory. To generate the desired trajectory, two different algorithms are presented (see, e.g., [8] and [12]) to seek the optimal velocity while ensuring the trajectory is sufficiently differentiable. In contrast to the linear approximation of the user force input required in previous research (e.g., [10] and [5]), the subsequent development does not require any model of the user torque input. Another goal of the controller is to ensure that the exercise machine remains passive with respect to the user's power input. To ensure passivity while also achieving trajectory tracking, two different controllers are developed. The first controller is developed based on the assumption that the user's torque input can be measured. Based on the desire to eliminate the need for force/torque sensors, a second controller is designed that estimates the user's torque input. Both controllers are proven to remain passive with respect to the user's power output and yield semiglobal tracking through Lyapunov-based analyses provided mild assumptions remain valid for the machine dynamics and the user input. Proof-of-concept experimental results are provided that illustrate the performance of the torque estimation controller.

The development described in this paper has several advantages over previous experiments. In comparison to the result in [5], the current result (as well as the results in [10] and [11]) does not require a one-sided mechanical braking mechanism to ensure passivity. In comparison to the results in [5], [10], and [11], the current development does not require a linear approximation of the Hill-based force-velocity curves. The proposed method does not require any model of the force-velocity curve. Eliminating the linear approximation is a significant challenge that requires a new method to determine the optimal trajectory of the exercise machine.

Manuscript received October 11, 2004; revised March 8, 2005. Recommended by Technical Editor R. Rajamani. This research was supported in part by National Science Foundation (NSF) under Grant DMI-9457967, Office of Naval Research (ONR) under Grant N00014-99-1-0589, a Department of Commerce (DOC) Grant, an Army Research Office (ARO) Automotive Center Grant, and in part by the Defence Advanced Research Project Agency (DARPA) through the Space Naval Warfare System Center, San Diego, under Contract N66001-03-R-8043.

X. T. Zhang and D. M. Dawson are with the Department of Electrical and Computer Engineering, Clemson University, Clemson, SC 29634-0915 USA (e-mail: xzhang@clemson.edu; ddawson@ces.clemson.edu).

W. E. Dixon is with the Department of Mechanical and Aerospace Engineering, University of Florida, Gainesville, FL 32611-6250 USA (e-mail: wdixon@ufl.edu).

B. Xian is with the Department of Mechanical and Materials Sciences, Duke University, Durham, NC 27705 USA (e-mail: xbin@duke.edu).

Digital Object Identifier 10.1109/TMECH.2006.871896

II. EXERCISE MACHINE DYNAMICS

While a variety of machine configurations are available to facilitate different exercises, many configurations can be reduced to a user torque input to an actuated motor. The model for a 1-degree of freedom (DOF) exercise machine is assumed to be as follows¹:

$$J\ddot{q}(t) = \tau(\dot{q}) + u(t) \quad (1)$$

where $J \in \mathbb{R}$ denotes the constant inertia of the machine, $q(t), \dot{q}(t), \ddot{q}(t) \in \mathbb{R}$ denote the angular position, velocity, and acceleration of the machine, respectively, $\tau(\dot{q}) \in \mathbb{R}$ denotes a velocity-dependent user torque input, and $u(t) \in \mathbb{R}$ denotes the motor control input. The user input is assumed to exhibit the following characteristics that are exploited in the subsequent development.

- Assumption 1*: The user input is a function of the machine velocity [i.e., $\tau(\dot{q})$].
- Assumption 2*: The user input is a second-order differentiable function [i.e., $\tau(\dot{q}) \in C^2$].
- Assumption 3*: The user input is unidirectional [i.e., assumed to be positive w.l.o.g. (without loss of generality)] and satisfies the following inequalities

$$0 \leq \tau(\dot{q}) \leq \tau_{\max} \quad (2)$$

where $\tau_{\max} \in \mathbb{R}$ is a positive constant denoting the maximum possible torque applied by the user.

- Assumption 4*: The desired trajectory is assumed to be designed such that $\dot{q}_d(t), \ddot{q}_d(t), \dddot{q}_d(t) \in \mathcal{L}_\infty$, where the desired velocity, denoted by $\dot{q}_d(t) \in \mathbb{R}$, is assumed to be in the same direction as the user input (i.e., assumed positive w.l.o.g.).²

Remark 1: In biomechanics literature, a user's joint torque is typically expressed as a function of position, velocity, and time [i.e., $\tau(q, \dot{q}, t)$]. The position dependence is related to the configuration of the limbs attached to the joint. As in [10], the user is assumed to be able to exert the same amount of torque throughout the required range-of-motion for the exercise, and hence, the position dependence can be neglected. The time dependence of the user's joint torque is due to the effects of fatigue (i.e., the amount of maximum torque diminishes as the user fatigues). As also described in [10], the user is assumed to maintain a constant level of fatigue during the exercise session, and hence, the time dependence can be neglected.

III. CONTROL DESIGN WITH MEASURABLE USER INPUT

A. Control Objectives

One objective of the exercise machine controller is to ensure that the exercise machine tracks a desired velocity. To quantify this objective, a velocity-tracking error, denoted by $e(t) \in \mathbb{R}$, is defined as

$$e(t) \triangleq \dot{q}(t) - \dot{q}_d(t) \quad (3)$$

where $\dot{q}_d(t) \in \mathbb{R}$ denotes a desired velocity that is assumed to be designed such that $\dot{q}_d(t), \ddot{q}_d(t), \dddot{q}_d(t) \in \mathcal{L}_\infty$. Another objective is to maximize the modified user power output, denoted by $p(\dot{q})$, that is defined as follows [10]:

$$p(\dot{q}) = \tau(\dot{q})\dot{q}^\rho(t) \quad (4)$$

¹Additional dynamic effects (e.g., friction) can be incorporated in the exercise machine model and subsequent control design. These terms have been neglected in the control development for simplicity.

²The assumption that $\dot{q}_d(t)$ is assumed to be positive is a similar assumption that is exploited in [10] and [11]. The assumption is considered to be mild since the trajectory generation algorithm can easily be restricted (e.g., a projection algorithm) to produce a positive value.

where $\rho \in \mathbb{R}$ is a positive constant³. To achieve this objective, the desired trajectory must also be designed to ensure that $\dot{q}_d(t) \rightarrow \dot{q}_d^*$ as $t \rightarrow \infty$, where $\dot{q}_d^* \in \mathbb{R}$ is a positive constant that denotes an unknown user-dependent optimal velocity setpoint. A final objective for the exercise machine controller is to ensure the safety of the user by guaranteeing that the machine remains passive with respect to the user's power input. The exercise machine is passive with respect to the user's power input provided the following integral inequality is satisfied [10]:

$$\int_{t_0}^t \tau(\sigma)\dot{q}(\sigma)d\sigma \geq -c^2 \quad (5)$$

where $c \in \mathbb{R}$ is a bounded positive constant.

Remark 2: In contrast to the linear approximation of the user force input required in [5] and [10], the subsequent development is based on a general form of the user torque input. Specifically, Assumptions 1–3 should be satisfied and $p(\dot{q})$ of (4) should have a global maximum for some value of $\dot{q}(t)$ (i.e., \dot{q}_d^*).

B. Control Development

The open-loop error system is determined by taking the time derivative of (3) and multiplying the result by J

$$J\dot{e}(t) = \tau(\dot{q}) + u(t) - J\ddot{q}_d(t) \quad (6)$$

where (1) has been utilized. In this section, the user torque input is assumed to be measurable. Based on this assumption, the structure of (6), and the subsequent stability analysis, the following controller is developed:

$$u(t) = -ke(t) + J\ddot{q}_d(t) - \tau(\dot{q}) \quad (7)$$

where $k \in \mathbb{R}$ is a positive constant control gain. After substituting (7) into (6), the following closed-loop error system can be determined:

$$J\dot{e}(t) = -ke(t). \quad (8)$$

C. Controller Analysis

Theorem 1: The exercise machine controller in (7) ensures that all system signals are bounded under closed-loop operation, and the velocity tracking error is exponentially stable in the sense that

$$e(t) = e(0) \exp\left(-\frac{k}{J}t\right). \quad (9)$$

Proof: See [14]. ■

Theorem 2: The controller in (7) ensures that the exercise machine is passive with respect to the user's power input.

Proof: By substituting (3) into (5), the following expression can be obtained:

$$\int_{t_0}^t \tau(\sigma)\dot{q}(\sigma)d\sigma = \int_{t_0}^t \tau(\sigma)e(\sigma)d\sigma + \int_{t_0}^t \tau(\sigma)\dot{q}_d(\sigma)d\sigma. \quad (10)$$

Based on Assumptions 3 and 4, it is clear that the right-most term in (10) is always positive; hence, since $e(t) \in \mathcal{L}_1$, (10) can be lower bounded

$$\int_{t_0}^t \tau(\sigma)e(\sigma)d\sigma \geq -\tau_{\max} \int_{t_0}^t |e(\sigma)|d\sigma = -c^2. \quad (11)$$

Based on (11), it is clear that the passivity condition given in (5) is satisfied. ■

³A discussion of the physical interpretation of ρ is provided in [10]

IV. DESIRED TRAJECTORY GENERATOR

In the previous development, it is assumed that a desired trajectory can be generated such that $\dot{q}_d(t), \ddot{q}_d(t), \dddot{q}_d(t) \in \mathcal{L}_\infty$, and that $\dot{q}_d(t) \rightarrow \dot{q}_d^*$, where \dot{q}_d^* is an unknown constant that maximizes the user power output. From (3) and (4), the user power output can be expressed as (where $\rho = 1$ w.l.o.g.)

$$p(e, t) = \tau(\dot{q}_d(t) + e(t))(\dot{q}_d(t) + e(t)). \quad (12)$$

Since Theorem 1 can be used to prove that $e(t) \rightarrow 0$ exponentially fast, (12) can be approximated as

$$p(t) \cong \tau(\dot{q}_d)\dot{q}_d(t). \quad (13)$$

From (13), it is clear that if $\dot{q}_d(t) \rightarrow \dot{q}_d^*$, then $p(t) \rightarrow \tau(\dot{q}_d^*)\dot{q}_d^*$, and hence, the user power output will be maximized. To generate a desired trajectory that ensures $\dot{q}_d(t), \ddot{q}_d(t), \dddot{q}_d(t) \in \mathcal{L}_\infty$, and that $\dot{q}_d(t) \rightarrow \dot{q}_d^*$, several extremum-seeking algorithms can be used. Two algorithms that can be used to generate the trajectory are described in the following sections.

A. Perturbation-Based Extremum Generation

For brevity, the extremum-seeking algorithm is simply presented along with a heuristic commentary on the internal workings of the algorithm as opposed to extensive mathematical efforts to prove convergence of the scheme. Specifically, following the work presented in [8], a saturated extremum algorithm for generating $\dot{q}_d(t)$ can be designed as

$$\begin{aligned} \dot{q}_d(t) &= a_e \sin(\omega t) + \hat{\theta}(t) \\ \dot{\hat{\theta}}(t) &= -\alpha_f \hat{\theta}(t) + \kappa(t) \\ \dot{\kappa}(t) &= -\alpha_0 \kappa(t) + \alpha_0 (k_{f1} \text{sat}(p) - \eta(t)) a_e \sin(\omega t) \\ \dot{\eta}(t) &= -k_{f2} \eta(t) + k_{f2} \text{sat}(p) \end{aligned} \quad (14)$$

where $a_e, \omega, \alpha_0, \alpha_f, k_{f1}$, and $k_{f2} \in \mathbb{R}$ are constant design parameters, $\hat{\theta}(t), \kappa(t)$, and $\eta(t)$ are filtered signals, and $\text{sat}(\cdot)$ denotes a continuous saturation function. The algorithm given in (14) reduces to the algorithm presented in [8] when the saturation functions are removed and $\alpha_f = 0$. These modifications to the algorithm are incorporated to ensure that $\dot{q}_d(t), \ddot{q}_d(t), \dddot{q}_d(t) \in \mathcal{L}_\infty$. The design parameters $a_e, \omega, \alpha_0, \alpha_f, k_{f1}$, and k_{f2} must be selected sufficiently small because the convergence analysis associated with (14) utilizes averaging techniques. Specifically, the convergence analysis requires that the cutoff frequency of the $\eta(t)$ filter used in (14) be lower than the frequency of the perturbation signal (i.e., ω). In fact, the convergence analysis requires that the closed-loop system exhibit three distinct time scales: i) high speed, the convergence of $e(t)$; ii) medium speed, the periodic perturbation parameter ω ; iii) slow speed, the filter parameter k_{f2} in the $\eta(t)$ dynamics. As presented in [8], the convergence analysis illustrates that an extremum algorithm similar to (14) finds a near-optimum solution (i.e., $\dot{q}_d(t)$ goes to some value very close to \dot{q}_d^*). With regard to the periodic terms in (14) [i.e., $\sin(\omega t)$ and $\cos(\omega t)$], an extremum-seeking scheme must “investigate” the neighborhood on both sides of the maximum. This investigation motivates the use of slow periodic terms in the algorithm.

B. Numerically Based Extremum Generation

As previously described, the algorithm in (13) can be used to show that if $\dot{q}_d(t) \rightarrow \dot{q}_d^*$, then the user power output will be maximized. An

extremum algorithm for generating $\dot{q}_d(t)$ was presented in (14); however, this algorithm can be slow to find \dot{q}_d^* . As an alternative to the approach given by (14), several numerically based extremum search algorithms (e.g., Brent’s method [12], Simplex method [12], etc.) can be used for the online computation of $\dot{q}_d(t)$. For example, Brent’s method requires measurement of only the output function [i.e., $p(t)$ in (4)] and two initial guesses that enclose the unknown value for \dot{q}_d^* (the two initial guesses are not required to be close to the value of \dot{q}_d^*). Brent’s method then uses an inverse parabolic interpolation algorithm and measurements of $p(t)$ to generate estimates for \dot{q}_d^* until the estimates converge. Specifically, the filter-based algorithm for computing $\dot{q}_d(t)$ is described in Appendix A.

V. CONTROL DESIGN WITHOUT MEASURABLE USER INPUT

The control development discussed in the previous section requires that the user torque input be measurable. To measure the user input, an additional sensor (i.e., a force/torque sensor) has to be included in the exercise machine design. Inclusion of the additional sensor results in additional cost and complexity of the system. Motivated by the desire to eliminate the additional sensor, the controller in this section is crafted by developing a nonlinear integral feedback term that produces a user torque input estimate.

A. Open-Loop Error System

To facilitate the subsequent development, a filtered tracking error, denoted by $r(t) \in \mathbb{R}$, is defined as

$$r(t) \triangleq \dot{e}(t) + \alpha_r e(t) \quad (15)$$

where $\alpha_r \in \mathbb{R}$ denotes a positive constant parameter. After differentiating (15) and multiplying both sides of the resulting equation by J , the following expression can be obtained:

$$J\dot{r}(t) = -e(t) + N(\dot{q}, \ddot{q}) + \dot{u}(t) - J\ddot{q}_d(t) \quad (16)$$

where the time derivative of (1) and (3) have been used, and the auxiliary function $N(\dot{q}, \ddot{q}) \in \mathbb{R}$ is defined as

$$N(\dot{q}, \ddot{q}) \triangleq \frac{d}{dt}[\tau(\dot{q})] + e(t) + J\alpha_r e(t). \quad (17)$$

To further facilitate the subsequent analysis, an auxiliary signal $N_d(t) \in \mathbb{R}$ is defined as

$$N_d(t) \triangleq N(\dot{q}, \ddot{q})|_{\dot{q}(t)=\dot{q}_d(t), \ddot{q}(t)=\ddot{q}_d(t)} \quad (18)$$

where (17) can be used to prove that $N_d(t), \dot{N}_d(t) \in \mathcal{L}_\infty$ based on the assumptions that $\dot{q}_d(t), \ddot{q}_d(t), \dddot{q}_d(t) \in \mathcal{L}_\infty$, and $\tau(\dot{q}) \in \mathcal{C}^2$. After adding and subtracting $N_d(t)$ to the right side of (16), the following expression can be obtained:

$$J\dot{r}(t) = -e(t) + \dot{u}(t) - J\ddot{q}_d(t) + \tilde{N}(\dot{q}, \ddot{q}) + N_d(t) \quad (19)$$

where $\tilde{N}(\dot{q}, \ddot{q}) \in \mathbb{R}$ is defined as

$$\tilde{N}(\dot{q}, \ddot{q}) \triangleq N(\dot{q}, \ddot{q}) - N_d(t). \quad (20)$$

Remark 3: Since $N(\dot{q}, \ddot{q})$ defined in (17) is continuously differentiable, $\tilde{N}(\dot{q}, \ddot{q})$ introduced in (20) can be upper bounded as indicated by the following inequality [13]:

$$|\tilde{N}(\dot{q}, \ddot{q}, t)| \leq \rho(\|z(t)\|)\|z(t)\| \quad (21)$$

where $z(t) \in \mathbb{R}^2$ is defined as

$$z(t) \triangleq [e(t) \quad r(t)]^T \quad (22)$$

and $\rho(\|z(t)\|) \in \mathbb{R}$ is a positive bounding function that is nondecreasing in $\|z(t)\|$.

B. Closed-Loop Error System

Based on the structure of (19) and the subsequent stability analysis, the following controller⁴ is developed:

$$\begin{aligned} u(t) = & J \ddot{q}_d(t) - [J \ddot{q}_d(t_0) - (k_s + 1)e(t_0)] \\ & - (k_s + 1)e(t) - \int_{t_0}^t (k_s + 1)\alpha_r e(\sigma) d\sigma \\ & - \int_{t_0}^t (\beta_1 + \beta_2) \text{sgn}(e(\sigma)) d\sigma \end{aligned} \quad (23)$$

where $\text{sgn}(\cdot)$ represents the standard signum function and $k_s, \beta_1, \beta_2 \in \mathbb{R}$ are positive control gains. The time derivative of (23) is given by

$$\dot{u}(t) = J \dddot{q}_d(t) - (k_s + 1)\dot{r}(t) - (\beta_1 + \beta_2) \text{sgn}(e(t)). \quad (24)$$

After substituting (24) into (19), the closed-loop dynamics for $r(t)$ can be determined

$$\begin{aligned} J\dot{r}(t) = & -e(t) - (k_s + 1)r(t) \\ & - (\beta_1 + \beta_2) \text{sgn}(e(t)) + \tilde{N}(\dot{q}, \ddot{q}) + N_d(t). \end{aligned} \quad (25)$$

C. Stability Analysis

Theorem 3: The exercise machine controller introduced in (23) ensures all signals are bounded under closed-loop operation and that

$$e(t), \dot{e}(t) \rightarrow 0 \quad \text{as } t \rightarrow \infty \quad (26)$$

provided the control gains β_1 and β_2 are selected according to the following sufficient conditions:

$$\beta_1 > |N_d(t)| + \frac{1}{\alpha_r} |\dot{N}_d(t)|, \quad \beta_2 > 0 \quad (27)$$

and the control gain k_s is selected sufficiently large with respect to the initial conditions of the system.

Proof: See Appendix B. ■

Remark 4: Since $e(t) \in \mathcal{L}_1$, similar arguments as provided in the proof for Theorem 2 can be utilized to conclude that the exercise machine controller in (23) is passive with respect the user power input.

D. Desired Trajectory Generator

The perturbation and numeric trajectory generators described previously could be used to generate a reference trajectory that ensures that $\dot{q}_d(t), \ddot{q}_d(t), \ddot{q}_d(t) \in \mathcal{L}_\infty$ with the exception that both methods depend on measurement of the user's power input $p(t)$. As indicated by (4), $p(t)$ is computed based on the assumption that the user torque input is measurable. Since the development in this section is based on the assumption that the user torque input is not measurable, a torque estimator, denoted by $\hat{\tau}(t) \in \mathbb{R}$, is constructed

$$\hat{\tau}(t) = -u(t) + J \ddot{q}_d(t) \quad (28)$$

where $u(t)$ is introduced in (23). Based on (28), the following lemma can be stated.

Lemma 1: The torque observer in (28) ensures that $\hat{\tau}(t) \in \mathcal{L}_\infty$ and $\tau(t) - \hat{\tau}(t) \rightarrow 0$ as $t \rightarrow \infty$ provided the control gains k_s, β_1 , and β_2 are selected according to Theorem 3.

⁴The bracketed terms in (23) are used to ensure that $u(0) = 0$.

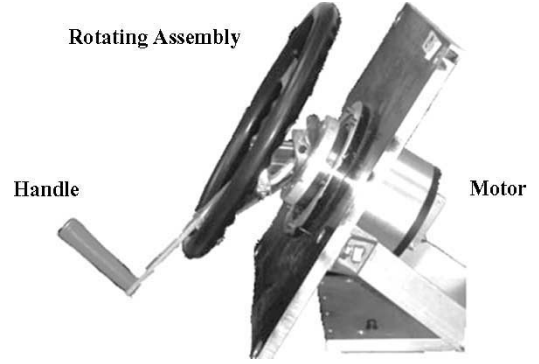


Fig. 1. Exercise machine testbed (side view).

Proof: Theorem 3 indicates that $u(t), e(t), \dot{e}(t) \in \mathcal{L}_\infty$, and $\dot{e}(t) \rightarrow 0$ as $t \rightarrow \infty$. The assumption that $\ddot{q}_d(t) \in \mathcal{L}_\infty$ and the facts that $u(t), \dot{e}(t) \in \mathcal{L}_\infty$ can be used along with (28) to show that $\hat{\tau}(t) \in \mathcal{L}_\infty$. After taking the time derivative of (3) and multiplying the result by J , the following expression is obtained:

$$\begin{aligned} J\dot{e}(t) = & J \ddot{q}(t) - J \ddot{q}_d(t) \\ = & \tau(t) - \hat{\tau}(t) \end{aligned} \quad (29)$$

where (1) and (28) have been used. By integrating both sides of (29)

$$\int_0^t (\tau(\sigma) - \hat{\tau}(\sigma)) d\sigma = J(e(t) - e(0)) \quad (30)$$

the facts that $e(t_0), e(t) \in \mathcal{L}_\infty$ can be used to show that $\tau(t) - \hat{\tau}(t) \in \mathcal{L}_1$. Based on the fact that $\dot{e}(t) \rightarrow 0$ as $t \rightarrow \infty$, (29) can also be used to conclude that $\tau(t) - \hat{\tau}(t) \rightarrow 0$ as $t \rightarrow \infty$. ■

Based on Lemma 1, the perturbation and numerically based extremum seeking algorithms can be rewritten where $p(t)$ is replaced by $\hat{\tau}(t)\dot{q}_d(t)$.

VI. EXPERIMENTAL RESULTS

The exercise machine testbed illustrated in Fig. 1 was constructed and used to complete experiments that illustrate the feasibility of using the proposed control strategy for maximizing the power expenditure of the user. As illustrated in Fig. 1, the exercise machine consisted of a handle that a user grasps; this handle is connected to a rotating assembly that is mounted on the rotor of a switched reluctance motor. The exercise machine testbed can be modeled by the single-input single-output nonlinear system introduced in (1). The inertia of the motor assembly was experimentally determined to be $J = 0.1 \text{ kg}\cdot\text{m}^2$. A resolver mounted on the motor is used to measure the rotor position while rotor velocity was calculated using a standard backward difference algorithm. The motor was interfaced with a Pentium IV PC operating under Microsoft Windows 2000. The control algorithm given in (23) was implemented in Simulink and converted to an executable file via the Real-Time Workshop and the dSpace Target. The executable file was loaded in the dSpace ControlDesk user interface for control parameter tuning and data logging and plotting.

To demonstrate the performance of the control algorithm given in (23), two experiments were conducted. For each experiment, a user held the handle of the exercise machine shown in Fig. 1 and rotated the motor shaft. Based on the desired angular velocity generated by the numerical-based extremum generation (Brent's method) algorithm, the controller given in (23) modifies the resistive torque output of the motor to maximize the user's power expenditure. Quantifying the

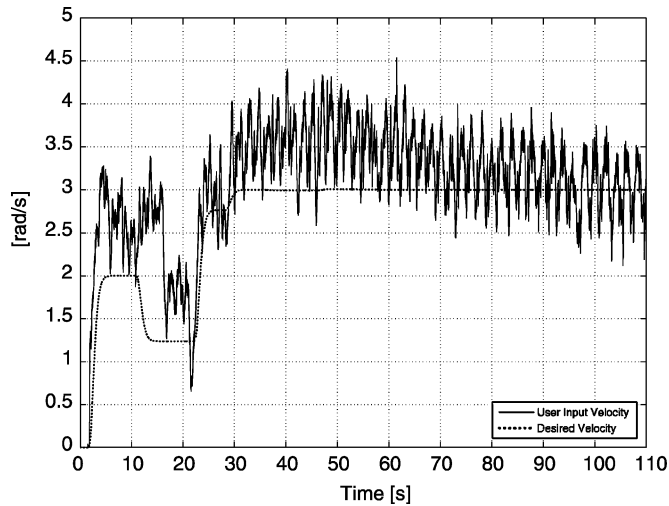


Fig. 2. Online computed velocity (dashed line) and achieved velocity (solid line).

ability of the exercise machine to find the maximum power expenditure of a user requires that the maximum be known. Since the maximum power output for some user is unknown, the first experiment exploits an artificial power function with a known maximum. Specifically, the following surrogate parabolic power function was utilized in the first experiment to generate $\dot{q}_d(t)$:

$$p(t) = 3 - \frac{1}{3}(\dot{q}_d(t) - 3)^2 \quad (31)$$

where it is clear that (31) is maximized at $\dot{q}_d^* = 3$ rad/s. That is, by using the surrogate input described in (31) to generate $\dot{q}_d(t)$, the ability of the extremum-seeking trajectory generator to accurately determine the maximum can be quantitatively tested.

To generate $\dot{q}_d(t)$ via Brent's method (see Appendix A), an initial estimate of the maximum $\dot{q}_d(t)$ is required (i.e., γ_2) along with lower and upper bounds (i.e., γ_1 and γ_3 , respectively). For the first experiment, γ_1 , γ_2 , and γ_3 were selected as follows:

$$\gamma_1 = 1 \quad \gamma_2 = 2.5 \quad \gamma_3 = 4.$$

To generate continuous bounded signals for $\dot{q}_d(t)$, $\ddot{q}_d(t)$, $\dddot{q}_d(t)$, the following stable and proper fourth-order filters were used:

$$\frac{d^i q_d}{dt^i} = \frac{81s^{i-1}}{s^4 + 12s^3 + 54s^2 + 108s + 81} \quad (32)$$

$\forall i = 1, 2, 3$. A 1.5-s time delay was used to allow for the torque estimate $\hat{\tau}(t)$ to converge to $\tau(t)$ before Brent's method is invoked. Fig. 2 illustrates that the desired exercise machine velocity converges to the optimal velocity setpoint (i.e., $\dot{q}_d^* = 3$ rad/s) and the actual velocity is achieved based on the following control gains:

$$k_s = 1 \quad \beta_1 + \beta_2 = 0.05 \quad \alpha_r = 0.05.$$

Fig. 3 depicts the control torque input $u(t)$.

In the first experiment, the desired exercise machine trajectory was generated via Brent's method, where $\tau(\dot{q}_d)$ was provided by a surrogate signal with a known maximum as a means to illustrate the ability of the extremum-seeking trajectory generator to converge to the desired maximum. In the second experiment, the surrogate signal was eliminated from the trajectory generator, allowing the desired trajectory to seek the

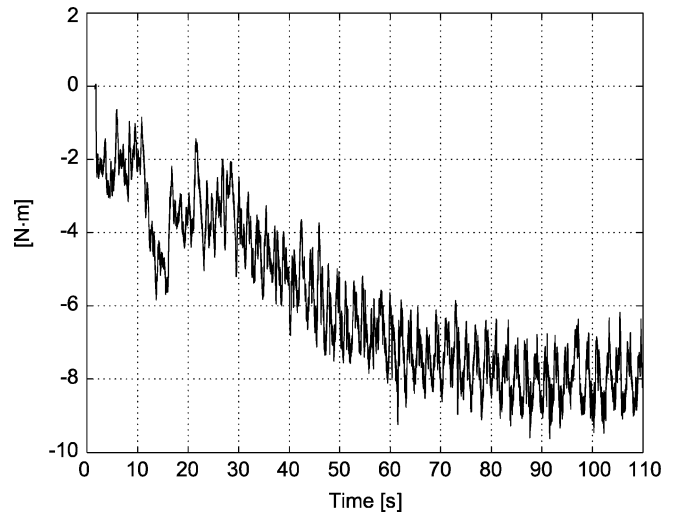


Fig. 3. Computed motor torque.

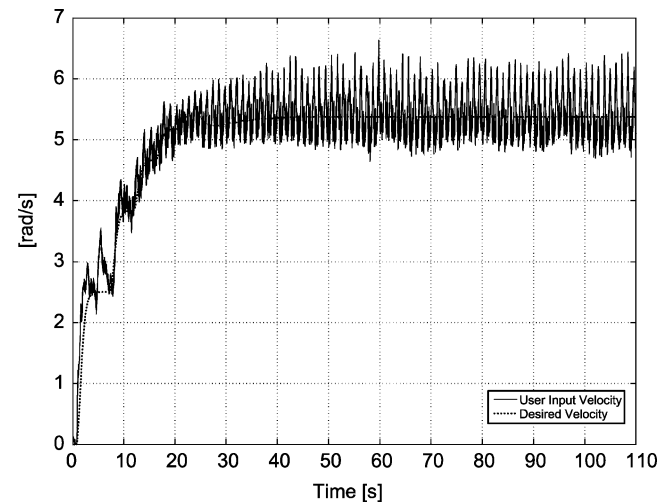


Fig. 4. Online computed velocity (dashed line) and achieved velocity (solid line).

maximum power expenditure of the user. For the second experiment, γ_1 , γ_2 , and γ_3 were selected as

$$\gamma_1 = 1 \quad \gamma_2 = 3.5 \quad \gamma_3 = 6.$$

The desired trajectory was constructed using the same filters given in (32), and a 1.5-s time delay was used to allow for the torque estimate $\hat{\tau}(t)$ to converge to $\tau(t)$. Fig. 4 depicts the online computed desired velocity and the actual velocity achieved based on the following control gains:

$$k_s = 2 \quad \beta_1 + \beta_2 = 0.1 \quad \alpha_r = 0.1.$$

Fig. 5 depicts the control torque input $u(t)$.

Remark 5: In [14], the control algorithm given in (23) was simulated for cases where the desired trajectory was generated by the perturbation-based extremum-seeking algorithm and the Brent's method. These results indicate the controller's performance in an ideal case. As shown in Figs. 2 and 4, the tracking error signals contain high-frequency components in practice and exhibit steady-state tracking errors of ± 0.5 (rad/s) and 1.0 to -0.5 (rad/s), respectively. The magnitude of the tracking errors may not be acceptable for typical tracking

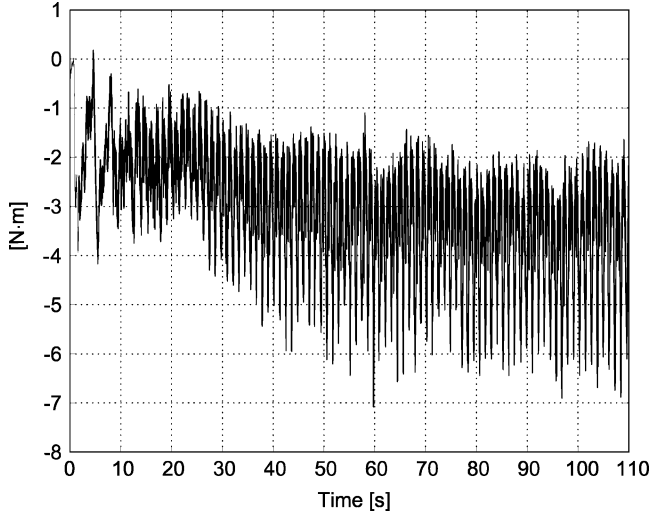


Fig. 5. Computed motor torque.

applications; however, this application is atypical since a human is directly interacting with the system in real-time. That is, the human input, denote by $\tau(\dot{q})$ in (1), can be viewed as an additive bounded disturbance that corrupts the tracking performance. While the high-frequency estimator given in (28) should theoretically compensate for this additive bounded disturbance, the actuator used in the experimental hardware has a limited bandwidth, and hence, some degradation in tracking performance can be expected. The simulation results in [14] also indicate that the time required by the perturbation-based extremum-seeking algorithm can be an order of magnitude greater than the time required to determine the extremum using Brent's method. Based on this fact, the perturbation-based extremum-seeking algorithm was not experimentally tested. The tracking performance presented in Figs. 2 and 4 are similar to the results obtained in [11].

VII. CONCLUSION

An exercise machine controller was developed that ensured passivity with the user. In an effort to optimize the user's power expenditure, two different desired velocity trajectory generators were provided that seek the unknown optimal velocity setpoint while ensuring the trajectory remains bounded and sufficiently differentiable. To track the desired trajectory and to ensure passivity, two controllers were developed. The first controller required the user's torque input to be measured, whereas the second controller estimated the user's torque input. Both controllers are proven to ensure that the exercise machine remained passive with respect to the user's power output. Each controller was proven to yield semiglobal tracking through Lyapunov-based analyses. The modified Brent's method extremum-seeking trajectory generator was used in conjunction with a nonlinear controller, which eliminated the need for force/torque measurement in the experiment. Proof-of-concept experimental results were provided and illustrated the performance of the desired trajectory generator and the torque estimation controller. The tracking performance was similar to the results obtained in [11].

APPENDIX A

NUMERICALLY BASED EXTREMUM GENERATION

The numerically based extremum generation formula for computing the optimal velocity setpoint that maximizes the user output power can be described as follows:

Step 1: Three initial best-guess estimates, denoted by $\gamma_1, \gamma_2, \gamma_3 \in \mathbb{R}$, are selected, where γ_1 is the best-guess estimate for a lower bound on the optimal velocity, γ_3 is the best-guess estimate for an upper bound on the optimal velocity, and γ_2 is the best-guess estimate for the optimal velocity, where $\gamma_2 \in (\gamma_1, \gamma_3)$.

Step 2: The lower bound estimate γ_1 is then passed through a set of third order stable and proper low-pass filters to generate continuous bounded signals for $\dot{q}_d(t), \ddot{q}_d(t), \dddot{q}_d(t)$. For example, the following filters could be used:

$$\begin{aligned}\dot{q}_d &= \frac{\varsigma_1}{s^3 + \varsigma_2 s^2 + \varsigma_3 s + \varsigma_4} \gamma_1 \\ \ddot{q}_d &= \frac{\varsigma_1 s}{s^3 + \varsigma_2 s^2 + \varsigma_3 s + \varsigma_4} \gamma_1 \\ \dddot{q}_d &= \frac{\varsigma_1 s^2}{s^3 + \varsigma_2 s^2 + \varsigma_3 s + \varsigma_4} \gamma_1\end{aligned}\quad (33)$$

where $\varsigma_1, \varsigma_2, \varsigma_3$, and ς_4 denote positive filter constants.

Step 3: Based on the result in (9), and the expressions for the user power output given in (12) and the structure in (33), the algorithm waits until $|e(t)| \leq \bar{e}_1$ and $|\dot{q}_d - \gamma_1| \leq \bar{e}_2$ before evaluating $p(\gamma_1)$, where \bar{e}_1 and \bar{e}_2 are some predefined threshold values.

Step 4: Steps 2 and 3 are repeated to obtain $p(\gamma_2)$ and $p(\gamma_3)$.

Step 5: The next desired trajectory point is determined from the following expression:

$$\gamma_4 = \gamma_2 - \frac{1}{2} \frac{g_1}{g_2} \quad (34)$$

where $g_1, g_2 \in \mathbb{R}$ are constants defined as

$$\begin{aligned}g_1 &= (\gamma_2 - \gamma_1)^2 [p(\gamma_2) - p(\gamma_3)] \\ &\quad - (\gamma_2 - \gamma_3)^2 [p(\gamma_2) - p(\gamma_1)]\end{aligned}\quad (35)$$

$$\begin{aligned}g_2 &= (\gamma_2 - \gamma_1) [p(\gamma_2) - p(\gamma_3)] \\ &\quad - (\gamma_2 - \gamma_3) [p(\gamma_2) - p(\gamma_1)]\end{aligned}\quad (36)$$

where γ_i and $p(\gamma_i), \forall i = 1, 2, 3$, are determined from steps 1–4. Specifically, γ_i and $p(\gamma_i)$ are substituted into (34)–(36) and the resulting expression yields the next best-guess for \dot{q}_d^* denoted by $\gamma_4 \in \mathbb{R}$.

Step 6: Steps 2 and 3 are repeated to obtain $\dot{q}_d(t), \ddot{q}_d(t), \dddot{q}_d(t)$ and $p(\gamma_4)$. Note that each successive estimate for \dot{q}_d^* produced by (34)–(36) will always be bounded by (γ_1, γ_3) , and hence, $\dot{q}_d(t), \ddot{q}_d(t), \dddot{q}_d(t) \in \mathcal{L}_\infty$.

Step 7: The value for $p(\gamma_4)$ is compared to $p(\gamma_2)$. If $p(\gamma_4) \geq p(\gamma_2)$ and $\gamma_2 > \gamma_4$ or if $p(\gamma_2) \geq p(\gamma_4)$ and $\gamma_4 > \gamma_2$, then the three new estimates used to construct a new parabola are γ_2, γ_3 , and γ_4 . If $p(\gamma_4) \geq p(\gamma_2)$ and $\gamma_4 > \gamma_2$ or if $p(\gamma_2) \geq p(\gamma_4)$ and $\gamma_2 > \gamma_4$, then the three new estimates used to construct a new parabola are γ_1, γ_2 , and γ_4 .

Step 8: Repeat steps 5–7 for successive $\gamma_i, \forall i = 5, 6, \dots$, where the three estimates determined from step 7 are used to construct a new parabola. Steps 5–7 are repeated until the difference between the new upper and lower estimates is below some predefined arbitrarily small threshold.

APPENDIX B

PROOF OF THEOREM 3

To prove the result in Theorem 3, the following lemmas are introduced.

Lemma 2: Let $L_1(t), L_2(t) \in \mathbb{R}$ be defined as

$$\begin{aligned} L_1(t) &\triangleq r(t)(N_d(t) - \beta_1 \text{sgn}(e(t))) \\ L_2(t) &\triangleq -\beta_2 \dot{e}(t) \text{sgn}(e(t)). \end{aligned} \quad (37)$$

If β_1 and β_2 introduced in (23) are selected to satisfy the sufficient conditions given in (27), then

$$\int_{t_0}^t L_1(\sigma) d\sigma \leq \zeta_{b1} \quad \int_{t_0}^t L_2(\sigma) d\sigma \leq \zeta_{b2} \quad (38)$$

where the positive constants $\zeta_{b1}, \zeta_{b2} \in \mathbb{R}$ are defined as

$$\zeta_{b1} \triangleq \beta_1 |e(t_0)| - e(t_0)N_d(t_0) \quad \zeta_{b2} \triangleq \beta_2 |e(t_0)|. \quad (39)$$

Proof: After substituting (15) into (37) and then integrating, the following expression is obtained:

$$\begin{aligned} \int_{t_0}^t L_1(\sigma) d\sigma &= \int_{t_0}^t \alpha_r e(\sigma) [N_d(\sigma) - \beta_1 \text{sgn}(e(\sigma))] d\sigma \\ &\quad + \int_{t_0}^t \frac{de(\sigma)}{d\tau} N_d(\sigma) d\sigma - \beta_1 \int_{t_0}^t \frac{de(\sigma)}{d\tau} \text{sgn}(e(\sigma)) d\sigma. \end{aligned} \quad (40)$$

Integrating the second integral on the right side of (40) by parts yields

$$\begin{aligned} &\int_{t_0}^t L_1(\sigma) d\tau \\ &= \int_{t_0}^t \alpha_r e(\sigma) (N_d(\sigma) - \beta_1 \text{sgn}(e(\sigma))) d\sigma \\ &\quad + e(\sigma) N_d(\sigma) \Big|_{t_0}^t - \int_{t_0}^t e(\sigma) \frac{dN_d(\sigma)}{d\tau} d\sigma - \beta_1 |e(\sigma)| \Big|_{t_0}^t \\ &= \int_{t_0}^t e(\sigma) \left(\alpha_r N_d(\sigma) - \frac{dN_d(\sigma)}{d\tau} - \alpha_r \beta_1 \text{sgn}(e(\sigma)) \right) d\sigma \\ &\quad + e(t) N_d(t) - e(t_0) N_d(t_0) - \beta_1 |e(t)| + \beta_1 |e(t_0)|. \end{aligned} \quad (41)$$

The expression in (41) can be upper bounded as follows:

$$\begin{aligned} \int_{t_0}^t L_1(\sigma) d\sigma &\leq \int_{t_0}^t |e(\sigma)| \left(\alpha_r |N_d(\sigma)| + \left| \frac{dN_d(\sigma)}{d\tau} \right| - \alpha_r \beta_1 \right) d\sigma \\ &\quad + |e(t)| (|N_d(t)| - \beta_1) \\ &\quad + \beta_1 |e(t_0)| - e(t_0) N_d(t_0). \end{aligned} \quad (42)$$

If β_1 is chosen according to (27), then the first inequality in (38) can be proven from (42). The second inequality in (38) can be obtained by integrating the expression for $L_2(t)$ introduced in (37) as follows:

$$\begin{aligned} \int_{t_0}^t L_2(\sigma) d\sigma &= \int_{t_0}^t (-\beta_2 \dot{e} \text{sgn}(e(t))) d\sigma \\ &= \beta_2 |e(t_0)| - \beta_2 |e(t)| \leq \beta_2 |e(t_0)|. \end{aligned} \quad (43)$$

Lemma 3: Consider the system $\dot{\xi} = f(\xi, t)$, where $f: \mathbb{R}^m \times \mathbb{R} \rightarrow \mathbb{R}^m$ for which a solution exists. Let the region \mathcal{D} be defined as $\mathcal{D} := \{\xi \in \mathbb{R}^m \mid \|\xi\| < \varepsilon\}$, where ε is some positive constant, and let $V: \mathcal{D} \times \mathbb{R} \rightarrow \mathbb{R}$ be a continuously differentiable function such that

$$W_1(\xi) \leq V(\xi, t) \leq W_2(\xi) \quad \text{and} \quad \dot{V}(\xi, t) \leq -W(\xi) \quad (44)$$

$\forall t \geq 0$ and $\forall \xi \in \mathcal{D}$, where $W_1(\xi), W_2(\xi)$ are continuous positive definite functions and $W(\xi)$ is a uniformly continuous positive semidefinite function. Provided (44) is satisfied and $\xi(0) \in \mathcal{S}$, we have

$$W(\xi(t)) \rightarrow 0 \quad \text{as} \quad t \rightarrow \infty \quad (45)$$

where the region denoted by \mathcal{S} is defined as follows:

$$\mathcal{S} := \{\xi \in \mathcal{D} \mid W_2(\xi) \leq \delta\} \quad \text{where} \quad \delta < \min_{\|\xi\|=\varepsilon} W_1(\xi) \quad (46)$$

and where δ denotes some positive constant.

Proof: Direct application of Theorem 8.4 in [9].

The proof for Theorem 3 can now be developed as follows.

Proof: Let $P_1(t), P_2(t) \in \mathbb{R}$ denote the following auxiliary functions

$$\begin{aligned} P_1(t) &= \zeta_{b1} - \int_{t_0}^t L_1(\sigma) d\sigma \\ P_2(t) &= \zeta_{b2} - \int_{t_0}^t L_2(\sigma) d\sigma \end{aligned} \quad (47)$$

where $\zeta_{b1}, \zeta_{b2}, L_1(t)$, and $L_2(t)$ are defined in Lemma 2. The results from Lemma 2 can be used to show that $P_1(t)$ and $P_2(t)$ are nonnegative. Let $V(y, t): \mathbb{R}^2 \times \mathbb{R} \times \mathbb{R} \times \mathbb{R}$ denote the following nonnegative function:

$$V(y, t) \triangleq \frac{1}{2} e^2(t) + \frac{1}{2} J r^2(t) + P_1(t) + P_2(t) \quad (48)$$

where $y(t) \in \mathbb{R}^2 \times \mathbb{R} \times \mathbb{R}$ is defined as

$$y(t) \triangleq \begin{bmatrix} z^T(t) & \sqrt{P_1(t)} & \sqrt{P_2(t)} \end{bmatrix}^T \quad (49)$$

and $z(t)$ was defined in (21). Since J is a positive constant, (48) can be lower and upper bounded by the following inequalities:

$$W_1(y) \leq V(y, t) \leq W_2(y) \quad (50)$$

where

$$W_1(y) = \lambda_1 \|y(t)\|^2 \quad W_2(y) = \lambda_2 \|y(t)\|^2 \quad (51)$$

and where $\lambda_1 \triangleq (1/2) \min\{1, J\}$ and $\lambda_2 \triangleq \max\{1, (1/2)J\}$.

After differentiating (48) and using (15), (25), (37), and the time derivative of (47), the following expression can be obtained:

$$\begin{aligned} \dot{V}(y, t) &= -\alpha_r e^2(t) - r^2(t) - k_s r^2(t) + r(t) \tilde{N}(\cdot) \\ &\quad - \beta_2 (\dot{e}(t) + \alpha_r e(t)) \text{sgn}(e(t)) + \beta_2 \dot{e}(t) \text{sgn}(e(t)) \\ &\leq -\lambda_3 \|z(t)\|^2 - k_s r^2(t) + r(t) \tilde{N}(\cdot) - \alpha_r \beta_2 |e(t)| \end{aligned} \quad (52)$$

where $\lambda_3 \triangleq \min\{1, \alpha_r\}$. By using (21), the following inequality can be developed:

$$\begin{aligned} \dot{V}(y, t) &\leq -\lambda_3 \|z(t)\|^2 - \alpha_r \beta_2 |e(t)| \\ &\quad + [r(t) |\rho(\|z(t)\|) \|z(t)\| - k_s r^2(t)]. \end{aligned} \quad (53)$$

■

Completing the squares on the bracketed term in (53) yields

$$\dot{V}(y, t) \leq - \left(\lambda_3 - \frac{\rho^2(\|z(t)\|)}{4k_s} \right) \|z(t)\|^2 - \alpha_r \beta_2 |e(t)|. \quad (54)$$

Based on (54), the following inequality can be developed

$$\dot{V}(y, t) \leq W(y) - \alpha_r \beta_2 |e(t)| \quad \text{for } k_s > \frac{\rho^2(\|z(t)\|)}{4\lambda_3}$$

$$\text{or } \|z(t)\| < \rho^{-1}(2\sqrt{\lambda_3 k_s}) \quad (55)$$

where

$$W(y) = -\gamma \|z\|^2 \quad (56)$$

and $\gamma \in \mathbb{R}$ is some positive constant. From (55) and (56), the regions \mathcal{D} and \mathcal{S} can be defined as

$$\mathcal{D} \triangleq \left\{ y \in \mathbb{R}^2 \times \mathbb{R} \times \mathbb{R} \mid \|y\| \leq \rho^{-1}(2\sqrt{\lambda_3 k_s}) \right\} \quad (57)$$

$$\mathcal{S} \triangleq \left\{ y \in \mathcal{D} \mid W_2(y) < \lambda_1 \left(\rho^{-1}(2\sqrt{\lambda_3 k_s}) \right)^2 \right\}. \quad (58)$$

The region of attraction in (58) can be made arbitrarily large to include any initial conditions by increasing the control gain k_s (i.e., a semiglobal stability result). Specifically, (51) and the region defined in (58) can be used to calculate the region of attraction

$$W_2(y(t_0)) < \lambda_1 \left(\rho^{-1}(2\sqrt{\lambda_3 k_s}) \right)^2$$

$$\implies \|y(t_0)\| < \sqrt{\frac{\lambda_1}{\lambda_2}} \rho^{-1}(2\sqrt{\lambda_3 k_s}) \quad (59)$$

which can be rearranged as

$$k_s > \frac{1}{4\lambda_3} \rho^2 \left(\sqrt{\frac{\lambda_2}{\lambda_1}} \|y(t_0)\| \right). \quad (60)$$

By using (15) and (49), the following explicit expression for $\|y(t_0)\|$ can be obtained:

$$\|y(t_0)\| = \sqrt{e^2(t_0) + (\dot{e}(t_0) + \alpha_r e(t_0))^2 + P_1(t_0) + P_2(t_0)} \quad (61)$$

where (1), (3), and the fact that $u(t_0) = 0$ can be used to determine that

$$\dot{e}(0) = J^{-1} \tau(t_0) - \ddot{q}_d(t_0).$$

From (48), (54), (55), and (58), it is clear that $V(y, t) \in \mathcal{L}_\infty \forall y(t_0) \in \mathcal{S}$; hence, $e(t), r(t), z(t), y(t) \in \mathcal{L}_\infty \forall y(t_0) \in \mathcal{S}$. From (55), it is also clear that $e(t) \in \mathcal{L}_1 \forall y(t_0) \in \mathcal{S}$. From (15), it can be shown that $\dot{e}(t) \in \mathcal{L}_\infty \forall y(t_0) \in \mathcal{S}$. Since $\ddot{q}_d(t)$ is assumed to be bounded, (23) can be used to prove that $u(t) \in \mathcal{L}_\infty \forall y(t_0) \in \mathcal{S}$. The previous boundedness statements can also be used along with (21), (25), and (56) to prove that $\dot{W}(y(t)) \in \mathcal{L}_\infty \forall y(t_0) \in \mathcal{S}$; hence, $W(y(t))$ is uniformly continuous. Lemma 3 can now be invoked to prove that $\|z(t)\| \rightarrow 0$ as $t \rightarrow \infty \forall y(t_0) \in \mathcal{S}$. Hence, (15) can be used to show that $e(t), \dot{e}(t), r(t) \rightarrow 0$ as $t \rightarrow \infty \forall y(t_0) \in \mathcal{S}$.

REFERENCES

- [1] G. A. Brooks and T. D. Fahey, *Exercise Physiology: Human Bioenergetics and its Applications*. New York: Wiley, 1984.
- [2] H. Kazerooni and M. G. Her, "A virtual exercise machine," in *Proc. 1993 Int. Conf. Robotics Autom.*, Atlanta, GA, May 1993, pp. 232–238.

- [3] T. Kjkuchi, J. Furusho, and K. Oda, "Development of isokinetic exercise machine using ER brake," in *Proc. 2003 IEEE Int. Conf. Robotics Autom.*, Taipei, Taiwan, Sep. 14–19, 2003, pp. 214–219.
- [4] M. S. de Queiroz, D. M. Dawson, S. Nagarkatti, and F. Zhang, *Lyapunov-Based Control of Mechanical Systems*. Cambridge: Birkhäuser, 2000.
- [5] J. Shields and R. Horowitz, "Controller design and experimental verification of a self-optimizing motion controller for smart exercise machines," in *Proc. Amer. Control Conf.*, Albuquerque, NM, Jun. 1997, pp. 2736–2742.
- [6] J. J. Slotine and W. Li, *Applied Nonlinear Control*. Englewood Cliffs, NJ: Prentice-Hall, 1991.
- [7] B. G. Nielsen, "Unfolding transitions in myosin give rise to the double-hyperbolic force-velocity relation in muscle," Quantum Protein Centre (QuP), Physics Institute, Tech. Univ. Denmark, Copenhagen.
- [8] M. Kristic and H. Deng, *Stabilization of Nonlinear Uncertain Systems*. New York: Springer-Verlag, 1998.
- [9] H. Khalil, *Nonlinear Systems*. Upper Saddle River, Englewood Cliffs, NJ: Prentice-Hall, 2002.
- [10] P. Y. Li, "Control of smart exercise machines—Part I: Problem formulation and nonadaptive control," *IEEE/ASME Trans. Mechatron.*, vol. 2, no. 4, pp. 237–247, Dec. 1997.
- [11] —, "Control of smart exercise machines—Part II: Self-optimizing control," *IEEE/ASME Trans. Mechatron.*, vol. 2, no. 4, pp. 248–258, Dec. 1997.
- [12] W. H. Press, S. A. Teukosky, W. T. Vetterly, and B. P. Flannery, *Numerical Recipes in Fortran, the Art of Scientific Computing*, 2nd ed. Cambridge, U.K. Cambridge Univ. Press, 1992.
- [13] B. Xian, M. S. de Queiroz, and D. M. Dawson, "A continuous control mechanism for uncertain nonlinear systems," in *Optimal Control, Stabilization, and Nonsmooth Analysis*. Heidelberg, Germany: Springer-Verlag, 2004, pp. 251–262.
- [14] X. T. Zhang, D. M. Dawson, W. E. Dixon, and B. Xian, (Mar. 2004), Extremum seeking nonlinear controllers for a human exercise machine, Clemson Univ. CRB Tech. Rep. [Online]. Available: <http://ece.clemson.edu/crb/publicn/tr.htm> CU/CRB/3/1/04/#1.

Application of a 3-DOF Parallel Manipulator for Earthquake Simulations

Erika Ottaviano and Marco Ceccarelli

Abstract—In this paper a formulation and experimental results are presented for a novel application of a 3-degree of freedom (DOF) parallel manipulator to simulate point seismograms and three-dimensional (3-D) earthquake motion. The rigid body acceleration is analyzed to simulate real 3-D earthquakes. Furthermore, first experimental results are reported to analyze earthquake effects on scaled civil structures.

Index Terms—Earthquake simulators, experimental robotics, parallel manipulators.

I. INTRODUCTION

Earthquake simulators are widely used in the field of Civil Engineering to investigate both earthquake characteristics and resistant constructions. Therefore, it is of great interest to have earthquake simulators that can reproduce earthquakes to test nature-scaled or scaled civil structures. Earthquake simulators are used in laboratories, like those referred in [1]–[3]. Those simulators do not operate for a three-dimensional (3-D) motion of the terrain due to earthquake waves. In

Manuscript received March 22, 2004; revised September 10, 2004. Recommended by Technical Editor M. Meng.

The authors are with LARM, University of Cassino, 03043 Cassino (Fr), Italy (e-mail: ottaviano@unicas.it; ceccarelli@unicas.it).

Digital Object Identifier 10.1109/TMECH.2006.871103